

Synthesis of Cr_2O_3 and Pt doped $\text{RuO}_2/\text{Bi}_2\text{O}_3$ Photocatalysts for Hydrogen Production from Water Splitting

S. H. Hsieh¹, G. J. Lee¹, S. H. Davies², S. J. Masten², J. J. Wu^{1,*}

¹Department of Environmental Engineering and Science, Feng Chia University, Taichung, 407, Taiwan

²Department of Environmental Engineering, Michigan State University, East Lansing, MI 48824, USA

Abstract This study focuses on the preparation of modified bismuth oxide photocatalysts using sonochemically assisted hydrothermal synthesis and photodeposition method. $\text{RuO}_2/\text{Bi}_2\text{O}_3$ photocatalysts were doped with Cr and Pt to enhance their photocatalytic activity. The crystalline phase compositions and surface structures of these photocatalysts were examined using SEM, TEM, XRD, and XPS. The photocatalytic performance of the Bi_2O_3 composites was evaluated in the presence or absence of oxalic acid, a sacrificial hole scavenger. According to our experimental results, visible-light-driven photocatalysis using our fabricated $\text{Cr}_2\text{O}_3/\text{Pt}/\text{RuO}_2:\text{Bi}_2\text{O}_3$ catalyst in the presence of oxalic acid results in a better rate of hydrogen evolution of up to $17.2 \mu\text{mol g}^{-1} \text{h}^{-1}$. A plausible mechanism for the photocatalytic splitting of water is also proposed.

Keywords Nano Photocatalyst, Water Splitting, Hydrogen Production, Bismuth Oxide

1. Introduction

Global climate change, peak oil demand, along with increasingly stringent air pollution regulations for combustion byproducts have necessitated the development of alternative fuels [1-3]. One alternative is the production of hydrogen gas by visible light-driven photocatalysis to split water into oxygen and hydrogen. In order to achieve technically and economically feasible using this process, highly efficient and cost-effective photocatalysts that use solar energy must be further developed [4]. These photocatalysts must be highly active under visible light irradiation ($\lambda > 400 \text{ nm}$), where most of the solar energy spectrum can be effectively utilized. While there has been much research on the development of these visible light-driven photocatalysts [5-8], much work still needs to be completed to develop such photocatalysts. Bismuth oxide can absorb visible light due to its narrow band gap, 2.8 eV. When bismuth oxide is modified with ruthenium oxides and platinum, the photocatalytic activity would enhance effectively [9]. In the current research, we have prepared a novel composite photocatalyst, $\text{Cr}_2\text{O}_3/\text{Pt}/\text{Bi}_2\text{O}_3:\text{RuO}_2$, which could utilize visible light photons and suppress the backward reaction of water re-formation from hydrogen and oxygen. In addition, oxalic acid was used as a sacrificing scavenger to

react with holes after electron photoexcitation and to evaluate its effect on hydrogen production.

2. Materials and Methods

In the study, all chemicals were purchased directly from the chemical company (Aldrich, Inc., USA). All chemicals used in this study were of the highest purity available and were used as received without further purification.

2.1. Synthesis of $\text{Cr}_2\text{O}_3/\text{Pt}/\text{RuO}_2:\text{Bi}_2\text{O}_3$

Six (6) g of $\text{Bi}(\text{NO}_3)_3$ were dissolved in 7.5 mL HNO_3 (1 M) to obtain an aqueous solution of Bi^{3+} , to which 4 g polyvinyl pyrrolidone (PVP) were added as a dispersant. Ruthenium trichloride ($\text{RuCl}_3 \cdot 3\text{H}_2\text{O}$, 10%) was specifically added to synthesize hybrid $\text{RuO}_2:\text{Bi}_2\text{O}_3$ catalysts, after which the color of the solution (or suspension) turned from white to black. Sodium hydroxide (4 M) was added to the Bi^{3+} aqueous solution under vigorous stirring, raising the pH to approximately 12, which resulted in the rapid precipitation of a white solid. After stirring for several minutes, the suspension was then irradiated with high-intensity ultrasound (600W, 20 kHz), where the temperature of the reaction mixture rose to 70°C . After irradiation, the precipitate was centrifuged and washed with alcohol and deionized water several times, and then dried at 60°C . The $\text{RuO}_2:\text{Bi}_2\text{O}_3$ catalyst was then calcined at 500°C for 2 hours.

Pt nanoparticles were anchored using photochemical deposition on the surface of the $\text{Bi}_2\text{O}_3:\text{RuO}_2$ photocatalyst.

* Corresponding author:
jjwu@fcu.edu.tw (J. J. Wu)

Published online at <http://journal.sapub.org/ajee>

Copyright © 2013 Scientific & Academic Publishing. All Rights Reserved

The as-synthesized photocatalyst (150 mg) was dispersed in 100 mL of distilled water using ultrasonic agitation for 1 hour. Following sonication, the suspension was transferred into a glass flask and a solution of 1:1 (v/v) water-methanol was added until the final volume was approximately 50 mL. Subsequently, 6 mM of $\text{H}_2\text{PtCl}_6 \cdot 6\text{H}_2\text{O}$ for platinum precursor was added while the suspension was stirred vigorously using a magnetic stirrer. Then the suspension was illuminated with a PenRay UV lamp (wavelength at 254 nm) for 2 hours to allow sufficient deposition of Pt. After illumination, the $\text{Pt}/\text{Bi}_2\text{O}_3\text{-RuO}_2$ was filtered and washed several times to remove excess chloride ions, and dried overnight at 80°C in the presence of oxygen. The doping of Cr_2O_3 on $\text{Pt}/\text{Bi}_2\text{O}_3\text{-RuO}_2$ was carried out using the photoreduction of Cr(VI) ions in the reactor as described by Maeda *et al.*[10]. The photoreactive suspension was formulated by dispersing 0.2 g of Bi_2O_3 , $\text{Bi}_2\text{O}_3\text{-RuO}_2$, or $\text{Pt}/\text{Bi}_2\text{O}_3\text{-RuO}_2$ in 400 mL of K_2CrO_4 solution (0.25 mM). After evacuation of oxygen, the solution was exposed to visible light ($\lambda > 400$ nm) at an intensity of 350 W Xe lamp for six hours to reduce Cr(VI) into Cr(III) . The temperature of the suspension was maintained at room temperature by a flow of cooling water bath during the preparation procedure. The final product was washed with distilled water and dried overnight at 60°C .

2.2. Characterization Instruments of Photocatalysts

The X-ray diffraction (XRD) patterns were recorded using RigakuUltima III diffractometer (Japan) with $\text{Cu-K}\alpha 1$ radiation, in the scan angle range from 10° to 80° . The morphologies of the catalysts were examined by using JEOL, JSM-7401F field emission scanning electron microscope (FE-SEM). High Resolution Transmission electron microscopic (HR-TEM) images recorded using JEOL JEM-2010 model. X-ray photoelectron spectroscopy (XPS) measurements were carried out using Physical Electronics PHI 5600 XPS instrument with monochromatic $\text{Al-K}\alpha$ as (1,486.6 eV) excitation source.

2.3. Evaluation of Photocatalytic Activity for Hydrogen Production from Water Splitting

The photocatalytic activity of Bi_2O_3 , $\text{Cr}_2\text{O}_3/\text{Bi}_2\text{O}_3$, $\text{Cr}_2\text{O}_3/\text{RuO}_2\text{-Bi}_2\text{O}_3$, and $\text{Cr}_2\text{O}_3/\text{Pt}/\text{RuO}_2\text{-Bi}_2\text{O}_3$ for the decomposition of distilled deionized (DDI) water (18 M Ω) using visible light was determined in the presence and absence of oxalic acid (0.03 M) as a hole scavenger. In the photocatalytic reaction process, the oxalic acids could play a role of being electron donor that can produce hydrogen simultaneously. Before illumination, helium was purged throughout the reactor to remove excess oxygen and the experiments were carried out at atmospheric conditions (25°C) and at neutral pH. The photocatalysts were irradiated by a 350 W Xe lamp, which emitted visible-light ($\lambda \geq 400$ nm) using a cutoff filter. The concentrations of H_2 and O_2 gases were determined using gas chromatography equipped with a thermal conductivity detector (Shimadzu Inc.). The

separation column was Mol Sieve 5A PLOT capillary column (Supelco Inc.), 30 m length and 0.53 mm i.d. with a 3.0 μm film thickness. Gas samples (0.5 mL) were injected into the GC. The flow rate of carrier gas, helium, was 3 mL/minute. The oven temperature was held at 50°C for 1 min and the temperature was then ramped at $20^\circ\text{C}/\text{min}$ to 100°C . Injector and detector temperatures were 150 and 180°C , respectively. The total run time for each sample was 4.5 minutes.

3. Results and Discussion

3.1. Characterization of Photocatalysts

The XRD spectra of $\text{Cr}_2\text{O}_3/\text{Pt}/\text{RuO}_2\text{-Bi}_2\text{O}_3$ prepared by photodeposition is presented in Figure 1, showing the characteristic peaks of Bi_2O_3 monoclinic structure at (121), (122), and (041) according to JCPDS Card File No. 71-2274. In addition, no other species were detected which indicates that crystalline impurities are not present. However, Cr_2O_3 peak was not detected by XRD spectra, although it was substantially identified using XPS as subsequently discussed. This may be due to the low loading amount (2.5% mass) at which it was added.

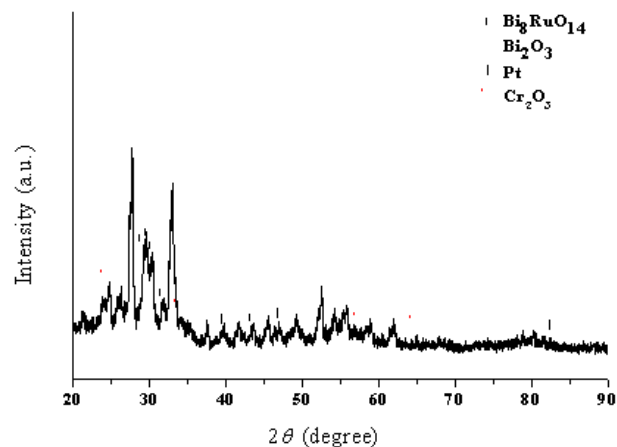


Figure 1. XRD pattern of Bi_2O_3 composites prepared in the solution with PVP

In this study, ruthenium oxide was firstly doped with bismuth oxide at around 10% (molar ratio). Subsequently, platinum and chromium oxide were deposited on the surface of the $\text{RuO}_2\text{-Bi}_2\text{O}_3$ photocatalyst as previously synthesized. SEM images in Figure 2 (a) and (b) reveal that the shape of bismuth oxides presented nanosheet and their surface was relatively smooth and the other elements, including ruthenium, platinum, and chromium nanoparticles, were precipitated homogeneously over the surface of bismuth oxide. The average nanoparticle size of $\text{Cr}_2\text{O}_3/\text{Pt}/\text{RuO}_2\text{-Bi}_2\text{O}_3$ photocatalyst was ranged at 100 nm approximately.

Structural analysis of the $\text{Cr}_2\text{O}_3/\text{Pt}/\text{RuO}_2\text{-Bi}_2\text{O}_3$ was performed using high-resolution transmission electron microscopy (HRTEM). The HRTEM image of

$\text{Cr}_2\text{O}_3/\text{Pt}/\text{RuO}_2:\text{Bi}_2\text{O}_3$ is shown in Figure 3(a). The HRTEM images of the region denoted in Figure 3(b) and 3(c) indicate the presence of Cr_2O_3 component indexed by an Energy Dispersive Spectrometer (EDS) analysis. The EDS analysis of a cross-section of $\text{Cr}_2\text{O}_3/\text{Pt}/\text{RuO}_2:\text{Bi}_2\text{O}_3$ photocatalyst has indicated the presence of bismuth, ruthenium, platinum, and chromium, respectively. In addition, the EDS maps (figure not shown) appear that chromium and ruthenium elements were dispersed homogeneously on the catalyst surface.

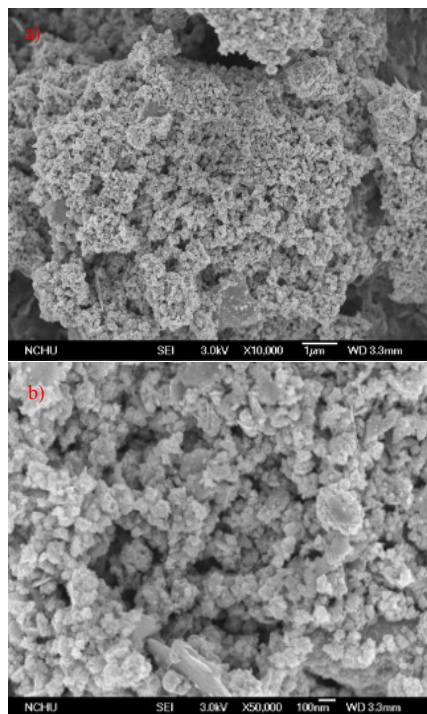


Figure 2. SEM images of $\text{Cr}_2\text{O}_3/\text{Pt}/\text{RuO}_2:\text{Bi}_2\text{O}_3$ photocatalyst

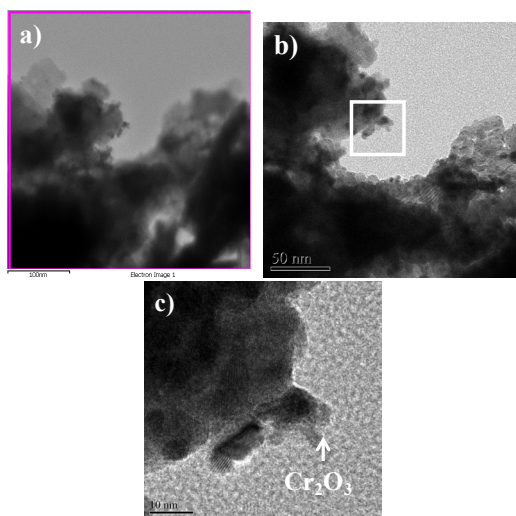
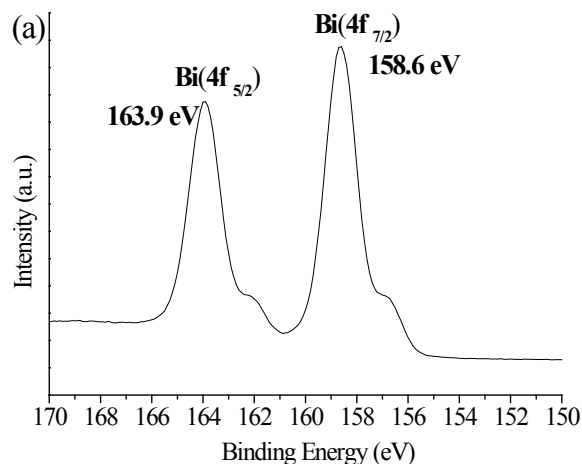
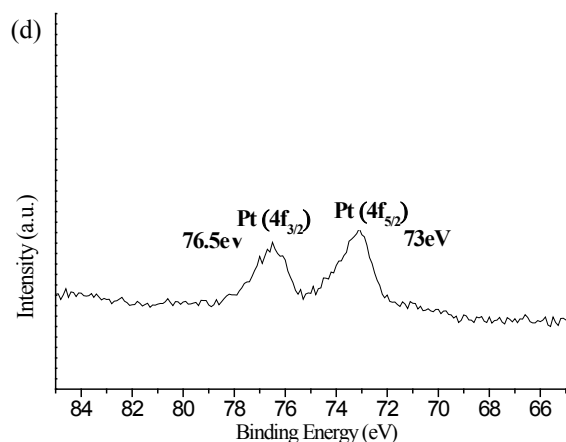


Figure 3. HRTEM images of (a) $\text{Cr}_2\text{O}_3/\text{Pt}/\text{RuO}_2:\text{Bi}_2\text{O}_3$, (b) and (c) Cr_2O_3 of the region denoted

To understand chemical states of the elements within the catalyst samples, XPS spectra analysis was performed to identify the chemical states of the elements in the catalyst in this research. The binding energies were corrected for

specimen charging by referencing them to the C1s peak at 284.8 eV. The quantitative analysis was done using XPS spectra obtained at the depth of about approximately 50 nm from the surface. Figure 4 shows XPS wide scans for the $\text{Cr}_2\text{O}_3/\text{Pt}/\text{RuO}_2:\text{Bi}_2\text{O}_3$ and elements of Bi, O, Ru, Cr, and Pt, respectively. The XPS spectra in Figure 4(a) revealed that the Bi species in the sample were present in the form of Bi_2O_3 , corresponding to the binding energy of pure Bi_2O_3 (158.6 eV and 163.9 eV) in Bi ($4f_{7/2}$) and Bi($4f_{5/2}$) levels, respectively[11]. Figure 4(b) shows that Ru peak located at 280.4 eV is consistent with Ru with a spin orbit splitting $3d_{5/2}-3d_{3/2}$ of 4.1 eV [see Ref 12 for spectrum]. The peak at 280.5 eV is consistent with that of metallic Ru, which has a binding energy of 280.0–280.3 eV. No other stable Rucations with an oxidation state lower than +4 are known to exist in the solid state[13]. The Cr2p peaks for $\text{Cr}_2\text{O}_3/\text{Pt}/\text{RuO}_2:\text{Bi}_2\text{O}_3$ appear at 577.2 eV ($2p_{3/2}$) and 586.7 eV ($2p_{1/2}$) as shown in Figure 4(c). The binding energies of $\text{Cr}_2\text{O}_3/\text{Pt}/\text{RuO}_2:\text{Bi}_2\text{O}_3$ are the typical binding energies of Cr $2p_{3/2}$ and Cr $2p_{1/2}$ for Cr_2O_3 , respectively[14]. The line bend in the vicinity of 576.3 eV is ascribed to Cr_2O_3 , indicating that chromium is present in the photocatalyst in the trivalent state. In addition, Figure 4(d) shows that the binding energy of Pt ($4f_{7/2}$) is found at 73 eV, which is similar to Pt^{2+} , and the Pt species are present in the ion state.



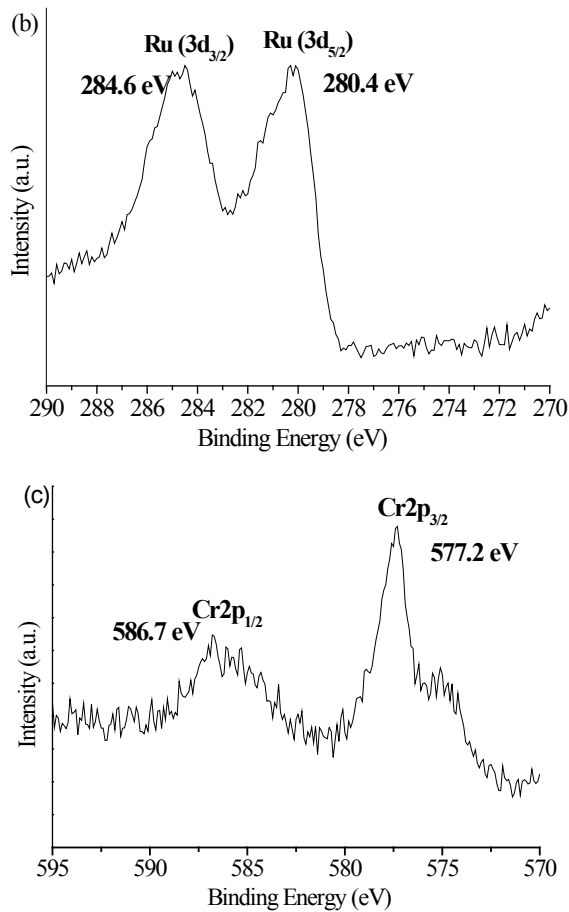


Figure 4. XPS spectra of survey for (a) Bi_{4f} , (b) Ru_{3d} , (c) Cr_{2p} , and (d) Pt_{4f}

3.2. Photocatalytic Activity of Photocatalysts

In order to compare the effect of adding oxalic acid into DDI water on hydrogen production, the experiment was conducted using $\text{Cr}_2\text{O}_3/\text{Pt}/\text{RuO}_2:\text{Bi}_2\text{O}_3$ as the photocatalyst. Figure 5 shows the H_2 evolution from the decomposition of water in the absence and presence of 0.03 M $\text{H}_2\text{C}_2\text{O}_4$ using visible light irradiation. It is apparent that the addition of oxalic acid resulted in more hydrogen production due to the donation of hole(h^+) scavenger. The formation amount of H_2 was estimated to be around $68.6 \mu\text{mol g}^{-1}$ in the presence of 0.03 M $\text{H}_2\text{C}_2\text{O}_4$ after 4 hours of irradiation on $\text{Cr}_2\text{O}_3/\text{Pt}/\text{RuO}_2:\text{Bi}_2\text{O}_3$. In Table 1, it is noted that the hydrogen production rate is ranked as the order of using $\text{Pt}/\text{RuO}_2:\text{Bi}_2\text{O}_3$, $\text{RuO}_2:\text{Bi}_2\text{O}_3$, and pristine Bi_2O_3 . The hydrogen production rate from water, involving 0.03 M of oxalic acid, reaches $17.2 \mu\text{mol/g-h}$ within 4 hours visible light irradiation in the presence of $\text{Pt}/\text{Cr}_2\text{O}_3/\text{RuO}_2:\text{Bi}_2\text{O}_3$ heterostructures and the result is obviously higher than the hydrogen production rate ($12.2 \mu\text{mol/g-h}$) in the presence of $\text{Cr}_2\text{O}_3/\text{RuO}_2:\text{Bi}_2\text{O}_3$ powder. Therefore, Pt nanoparticles should play an important role in hydrogen production and Pt nanoparticles act as electron traps, thereby improving the separation of photoexcited electrons and holes and resulting in a decrease in the recombination opportunities. Although $\text{Pt}/\text{RuO}_2:\text{Bi}_2\text{O}_3$ has shown a good photocatalytic activity for overall water

splitting, backward reaction of water still continuously suppresses hydrogen production and most likely due to rapid water formation on the Pt nanoparticles [15]. Therefore, the suppression of water re-formation is essential to achieve efficient evolution of H_2 and O_2 in the photocatalysis system. Table 1 also lists the photocatalytic activities for visible-light-driven hydrogen production by Bi_2O_3 , $\text{RuO}_2:\text{Bi}_2\text{O}_3$, and $\text{Pt}/\text{RuO}_2:\text{Bi}_2\text{O}_3$ before and after photodeposition of Cr_2O_3 . When photodeposition of Cr_2O_3 upon these catalysts were employed, the rate of hydrogen evolution increased. A 20% enhancement in hydrogen evolution was observed with $\text{Cr}_2\text{O}_3/\text{Pt}/\text{RuO}_2:\text{Bi}_2\text{O}_3$ as compared with $\text{Pt}/\text{RuO}_2:\text{Bi}_2\text{O}_3$. From these results, it demonstrates that chromium oxide modified Bi_2O_3 composites can improve the amount of hydrogen evolution. The results of doping Cr_2O_3 strongly suggest that Cr_2O_3 suppress water reformation from H_2 and O_2 on noble metals, thereby allowing for the forward reactions [16]. In this system, the backward reaction over the noble metal is effectively prevented by the Cr_2O_3 because it can permeable to protons and evolved H_2 molecules, but not to O_2 [17]. This is consistent with the findings of Maeda *et al.* [18] who reported that the reduction of H^+ into H_2 occurs on the Cr_2O_3 . In addition, Cr_2O_3 has the ability to adsorb H^+ and to activate the H atom. The amount of oxygen (on a molar basis) that evolved from water splitting was approximately half of the hydrogen production (data not shown), which is consistent with the chemical structure of water molecules.

Table 1. Photocatalytic activity for visible-light-driven water splitting on different photocatalysts modified with Cr_2O_3 in the presence of 0.03 M oxalic acid

Photocatalysts	Cr_2O_3 photodeposition	Activity [$\mu\text{mol g}^{-1} \text{h}^{-1}$] H_2
Bi_2O_3	no	8.9 ± 1.1
Bi_2O_3	yes	9.3 ± 0.8
$\text{RuO}_2:\text{Bi}_2\text{O}_3$	no	11.8 ± 2.4
$\text{RuO}_2:\text{Bi}_2\text{O}_3$	yes	12.2 ± 3.2
$\text{Pt}/\text{RuO}_2:\text{Bi}_2\text{O}_3$	no	14.5 ± 0.9
$\text{Pt}/\text{RuO}_2:\text{Bi}_2\text{O}_3$	yes	17.2 ± 1.3

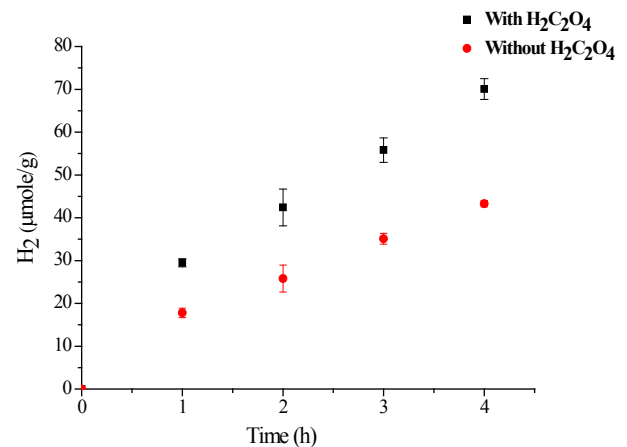


Figure 5. Changes in hydrogen evolution amount by visible-light-driven photocatalyst of $\text{Cr}_2\text{O}_3/\text{Pt}/\text{RuO}_2:\text{Bi}_2\text{O}_3$ with and without the addition of 0.03 M $\text{H}_2\text{C}_2\text{O}_4$ in water

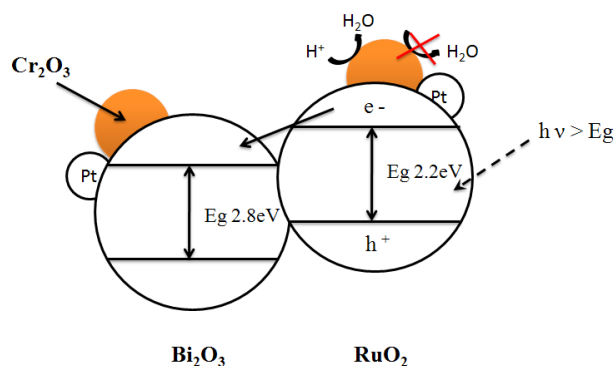
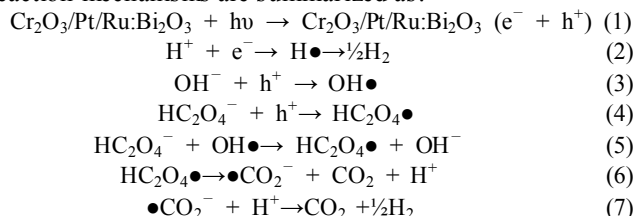


Figure 6. The plausible mechanism of H_2 evolution on Cr_2O_3 in photocatalytic water splitting

The reaction mechanisms of H_2 evolution on noble metal nanoparticles in photocatalytic water splitting can be illustrated in Figure 6. From the mention above, Cr_2O_3 would contribute to the better performance as a cocatalyst for photocatalytic H_2 evolution. Hydrogen production in the presence of oxalic acid is initiated by photoexcitation to form electron-hole pairs. The photogenerated electron (e^-) can be transferred to electron acceptor H^+ . With Pt doped on $Cr_2O_3/Pt/RuO_2:Bi_2O_3$ catalyst, Pt can trap electrons and hydrogen gas can be thus produced on Pt. Likewise, holes can be filled by electron donors, such as $C_2O_4^{2-}$, $HC_2O_4^-$, $H_2C_2O_4$, and surface hydroxyl groups on $Cr_2O_3/Pt/RuO_2:Bi_2O_3$, respectively. According to ref.[17,19], the plausible reaction mechanisms are summarized as:



4. Conclusions

$Cr_2O_3/Pt/RuO_2:Bi_2O_3$ was successfully synthesized using a sonochemical method at about $70^\circ C$. HRTEM results show that the composite consists of RuO_2 and Bi_2O_3 nanoparticles and the particle size is about 100 nm after calcinations. Platinum and Cr_2O_3 nanoparticles are deposited on the surface of Bi_2O_3 via photodeposition method using HRTEM analysis. XPS has also presented the presence of Bi, O, Ru, Cr, and Pt, corresponding to Bi_2O_3 , RuO_2 , Cr_2O_3 , and metallic Pt. $Cr_2O_3/Pt/RuO_2:Bi_2O_3$ catalyst has been fabricated to develop the excellent photocatalytic activity for hydrogen production from water containing oxalic acid as holes scavengers under visible light irradiation. The rate of hydrogen evolution of $Cr_2O_3/Pt/RuO_2:Bi_2O_3$ with the addition of 0.03 M $H_2C_2O_4$ is about $17.2 \mu mol\ g^{-1}\ h^{-1}$.

ACKNOWLEDGEMENTS

The authors wish to thank for the financial support from

National Science Council in Taiwan under the contract number of NSC-100-2632-E-035-001-MY3 and Michigan State University for the visiting scholar appointment.

REFERENCES

- [1] Moriarty P., Honnery D., "Hydrogen's Role in an Uncertain Energy Future", International Journal of Hydrogen Energy, Vol. 34, Issue 1, pp. 31-39, 2009.
- [2] Elama C.C., Sandrock G., Luzzi A., Lindblad P., Hagen E.F., "Realizing the Hydrogen Future: the International Energy Agency's Efforts to Advance Hydrogen Energy Technologies", International Journal of Hydrogen Energy, Vol. 28, No. 6, pp. 601-607, 2003.
- [3] Balat M., "Potential Importance of Hydrogen as a Future Solution to Environmental and Transportation Problems", International Journal for Hydrogen Energy, Vol. 33, Issue 15, pp. 4013-4029, 2008.
- [4] Hu Y.C., Guo P.H., Guo L.J., "Synthesis and Photocatalytic Properties of Cr-doped $KSr_2Nb_3O_{10}$ for Hydrogen Production", International Journal of Hydrogen Energy, Vol. 37, Issue 1, pp. 1007-1013, 2012.
- [5] Maeda K., Domen K., "Surface Nanostructures in Photocatalysts for Visible-Light-Driven Water Splitting", Topics in Current Chemistry, Vol. 303, pp. 95-119, 2011.
- [6] Holladay J.D., Hu J., King D.L., Wang Y., "An Overview of Hydrogen Production Technologies", Catalysis Today, Vol. 139, Issue 4, pp. 244-260, 2009.
- [7] Zhu J., Zäch M., "Nanostructured Materials for Photocatalytic Hydrogen Production", Current Opinion in Colloid & Interface Science, Vol. 14, Issue 4, pp. 260-269, 2009.
- [8] Etheridge D.M., Steele L.P., Langenfelds R.L., Francey R.J., Barnola J.M., Morgan V.I., "Natural and Anthropogenic Changes in Atmospheric CO_2 over the Last 1000 Years from Air in Antarctic Ice and Firn", Journal of Geophysical Research: Atmosphere, Vol. 101, pp. 4115-4128, 1996.
- [9] Hsieh S.H. Master dissertation, Department of Environmental Engineering and Science, Feng Chia University, Taiwan; 2011.
- [10] Maeda K., Sakamoto N., Ikeda T., Ohtsuka H., Xiong A., Lu D., Kanehara M., Teranishi T., Domen K., "Preparation of Core-Shell-Structured Nanoparticles (with a Noble-Metal or Metal Oxide Core and a Chromia Shell) and Their Application in Water Splitting by Means of Visible Light", Chemistry - A European Journal, Vol. 16, Issue 26, pp. 7750-7759, 2010.
- [11] Irmawati R., Noorfarizan Nasriah, M.N., Taufiq-Yap Y.H., Abdul Hamid S.B., "Characterization of Bismuth Oxide Catalysts Prepared from Bismuth Trinitrate Pentahydrate: Influence of Bismuth Concentration", Catalysis Today, Vol. 93-95, Issue 1, pp. 701-709, 2004.
- [12] Fruth V., Popa M., Berger D., Ionica C.M., Jitianu M., "Phases investigation in the antimony doped Bi_2O_3 system", Journal of the European Ceramic Society, Vol. 24, Issue 6, pp. 1295-1299, 2004.
- [13] Zhu J., Wang S., Wang J., Zhang D., Li H., "Highly Active

- and Durable $\text{Bi}_2\text{O}_3/\text{TiO}_2$ Visible Photocatalyst in Flower-Like Spheres with Surface-Enriched Bi_2O_3 Quantum Dots”, *Applied catalysis. B, Environmental*, Vol. 102, No.1-2, pp. 120-125, 2011.
- [14] Madhavaram H., Idriss H., Wendt S., Kim Y.D., Knapp M., Over H., Abmann J., Löffler E., Muhler M., “Oxidation Reactions over RuO_2 : A Comparative Study of the Reactivity of the (110) Single Crystal and Polycrystalline Surfaces”, *Journal of Catalysis*, Vol. 202, Issue 2, pp. 296-307, 2001.
- [15] Maeda K., Domen K., “Photocatalytic Water Splitting: Recent Progress and Future Challenges”, *The Journal of Physical Chemistry Letters*, Vol. 1, No. 18, pp. 2655-2661, 2010.
- [16] Busca G., “Fourier Transform-infrared Spectroscopic Study of the Adsorption of Hydrogen on Chromia and on Some Metal Chromites”, *Journal of Catalysis*, Vol. 120, Issue 2, pp. 303-313, 1989.
- [17] Li Y.X., Lu G.X., Li S.B., “Photocatalytic Hydrogen Generation and Decomposition of Oxalic acid over Platinized TiO_2 ”, *Applied Catalysis A: General*, Vol. 214, Issue 2, pp. 179-185, 2001.
- [18] Maeda, K., Teramura, K., Lu, D., Saito, N., Inoue, Y., Domen, K. “Roles of $\text{Rh/Cr}_2\text{O}_3$ (Core/Shell) Nanoparticles Photodeposited on Visible-Light-Responsive $(\text{Ga}_{1-x}\text{Zn}_x)(\text{N}_{1-x}\text{O}_x)$ Solid Solutions in Photocatalytic Overall Water Splitting”, *Journal of Physical Chemistry C*, Vol. 111, pp. 7554-7560, 2007.
- [19] Song S., Tu J.J., Xu L.J., Xu X., He Z.Q., Qiu J.P., Ni J.G., Chen J.M., “Preparation of a Titanium Dioxide Photocatalyst Codoped with Cerium and Iodine and its Performance in the Degradation of Oxalic Acid”, *Chemosphere*, Vol. 73, Issue 9, pp. 1401-1406, 2008.